JOC Article
pubs.acs.org/joc

Effect of Transition State Aromaticity and Antiaromaticity on Intrinsic Barriers of Proton Transfers in Aromatic and Antiaromatic Heterocyclic Systems; An *ab Initio* Study

Claude F. Bernasconi* and Philip J. Wenzel

Department of Chemistry and Biochemistry, University of California, Santa Cruz, California 95064, United States

bernasconi@chemistry.ucsc.edu

Received August 31, 2010

EARLY DEVELOPMENT OF AROMATICITY AND LATE DEVELOPMENT OF ANTIAROMATICITY AT THE TRANSITION STATE LOWERS BARRIERS

An *ab initio* study of two series of carbon-to-carbon proton transfer reactions is reported. The first series refers to the heterocyclic $C_4H_5X^+/C_4H_4X$ (X = CH^-, NH, S, O, PH, CH_2, AlH, BH) systems, and the second to the linear 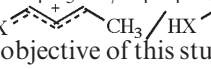 (X = CH^-, NH, S, PH, O, CH_2, AlH, BH) reference systems . The major objective of this study was to examine to what degree the aromaticity of C_4H_4X (X = CH^-, NH, S, O, PH) and the antiaromaticity of C_4H_4X (X = AlH, BH) is expressed at the transition state of the proton transfer and how this affects the respective intrinsic barriers. From the differences in the barriers between a given cyclic system and the corresponding linear reference system , $\Delta\Delta H^{\ddagger} = \Delta H^{\ddagger}$(cyclic) − $\Delta H^{\ddagger}$(linear), it was inferred that in the cyclic systems both aromaticity and antiaromaticity lower $\Delta H^{\ddagger}$(cyclic). This conclusion was based on the assumption that the factors *not* associated with aromaticity or antiaromaticity such as resonance, inductive and polarizability effects in the protonated species, and charge delocalization occurring along the reaction coordinate affect $\Delta H^{\ddagger}$ for the cyclic and linear systems in a similar way and hence offset each other in $\Delta\Delta H^{\ddagger}$. The extent by which $\Delta H^{\ddagger}$(cyclic) is lowered in the aromatic systems correlates quite well with the degree of aromaticity of C_4H_4X as measured by aromatic stabilization energies as well as the NICS(1) values of the respective C_4H_4X. According to the rules of the principle of nonperfect synchronization (PNS), these results imply a disproportionately large degree of aromaticity at the transition state for the aromatic systems and a disproportionately small degree of transition state antiaromaticity for the antiaromatic systems. These conclusions are consistent with the changes in the NICS(1) values along the reaction coordinate. Other points discussed in the paper include the complex interplay of resonance, inductive, and polarizability effects, along with aromaticity and antiaromaticity on the proton affinities of C_4H_4X.

Introduction

It is now generally recognized that the most appropriate kinetic measure of chemical reactivity is the *intrinsic* barrier or *intrinsic* rate constant[1−3] because it is not affected by the thermodynamic driving force of the reaction. For this reason a major focus of the research in our laboratory over the past 25 years has been on determining the factors that affect intrinsic barriers. More specifically, we have examined to what extent a variety of product or reactant stabilizing (destabilizing) factors are expressed at the transition state of reactions and how this influences intrinsic barriers. A most useful framework for the discussion and understanding of

(1) The intrinsic barrier of a reaction with a forward rate constant k_1 and a reverse rate constant k_{-1} is defined as $\Delta G_o^{\ddagger} = \Delta G_1^{\ddagger} = \Delta G_{-1}^{\ddagger}$ when $\Delta G^{\circ} = 0$;[2,3] the intrinsic rate constant is defined as $k_o = k_1 = k_{-1}$ when $K_1 = k_1/k_{-1} = 1$; in the gas phase the intrinsic barrier is usually defined as $\Delta H_o^{\ddagger} = \Delta H_1^{\ddagger} = \Delta H_{-1}^{\ddagger}$ when $\Delta H^{\circ} = 0$.

(2) Marcus, R. A. *J. Phys. Chem.* **1968**, *72*, 891.

(3) Keeffe, J. R.; Kresge, A. J. In *Investigation of Rates and Mechanisms of Reactions*; Bernasconi, C. F., Ed.; Wiley-Interscience: New York, 1986; Part 1, p 747.

Published on Web 11/16/2010 DOI: 10.1021/jo101719z

such effects has been the principle of nonperfect synchronization (PNS).[4] It states that any product stabilizing factor whose development at the transition state lags behind bond changes ("imbalanced" transition state) increases the intrinsic barrier, whereas a product stabilizing factor whose development is more advanced than bond changes reduces the intrinsic barrier; in the case of synchronicity of the two events ("balanced" transition state), there is no change in the intrinsic barrier. Also note that a factor whose development lags behind (is ahead of) bond changes in the forward direction of a reaction is lost early (late) in the reverse direction. This principle is mathematically provable, and hence there can be no exception. Appropriate modifications are equally applicable to *reactant* stabilizing factors[5a] and to product and reactant *de*stabilizing factors.[5b]

Studies of proton transfers from carbon acids activated by π-acceptor groups have played a prominent role in illustrating the various manifestations of the PNS.[4,6−9] Until recently, the major focus has been on how resonance/charge delocalization, solvation, inductive effects, and polarizability effects affect intrinsic barriers and can be understood in the context of the PNS. These effects may be briefly summarized as follows:

1. Resonance/Charge Delocalization. Charge delocalization always lags behind proton transfer[4−10] at the transition state, or in the reverse direction, charge localization is more advanced than proton transfer. This is illustrated, in exaggerated form, for the deprotonation of a nitroalkane in reaction 1. According to the PNS this kind of transition state imbalance invariably leads to an increase in the intrinsic barrier and the more so the stronger the resonance stabilization of the carbanion.

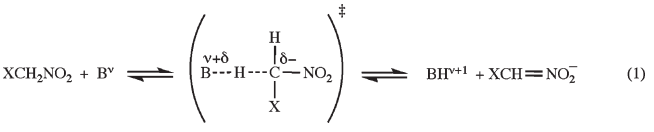

(1)

2. Solvation. Solvation of the carbanion also invariably lags behind proton transfer, which results in a further increase in the intrinsic barrier.[4,11] This effect is particularly strong when the carbanionic charge ends up mainly on an oxygen atom as is the case for nitronate or enolate ions and solvation is by hydrogen bonding in a protic solvent.

3. Inductive Effects. In proton transfers with an imbalanced transition state, inductive effects may either increase or decrease the intrinsic barrier. For example, an electron-withdrawing substituent X in reaction 1 lowers the intrinsic barrier. This is the result of a disproportionately strong stabilization of the transition state by X relative to that of the anion because the developing charge is closer to the substituent at the transition state than in the carbanion. However, in reaction 2 an electron-withdrawing substituent X would *increase* the intrinsic barrier because in this case X is closer to the charge in the product ion than in the transition state and hence it is the product that enjoys a disproportionately strong stabilization. Note that in the absence of a transition state imbalance the inductive effect would not affect the *intrinsic* barrier, although it probably would affect the *actual* barrier.

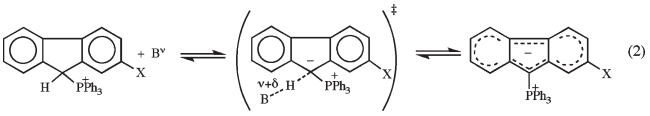

(2)

4. Polarizability Effects. A polarizable group adjacent to the reaction site (e.g., X in reaction 1) stabilizes the negative charge at the transition state but has little effect on the much more remote charge in the anion.[14] This leads to a reduction of the intrinsic barrier. Conversely, a polarizable X group in reaction 2 would have hardly any effect on the transition state but stabilizes the anion, thereby increasing the intrinsic barrier.[14] Similar polarizability effects operate in reactions involving cationic charges as is the case in the present study (see below).

More recently our interest has turned to the potential reactant or product stabilizing effect of aromaticity on intrinsic barriers. Our initial working hypothesis was that, inasmuch as aromaticity and resonance are related, the development of product aromaticity at the transition state should be expected to lag behind proton transfer and, just as is the case for resonance effects, should increase the intrinsic barrier. Experimental[16] as well as computational results[17] from our laboratory suggest that our working hypothesis was wrong: aromaticity *reduces* intrinsic barriers, which according to the PNS implies that the development of product aromaticity at the transition state is more advanced than proton transfer. The largest reductions in the intrinsic barrier have been noted for the gas-phase carbon-to-carbon identity proton transfers shown in reactions 3a and 4a.[17a] On the basis of comparisons with the respective noncyclic

(4) (a) Bernasconi, C. F. *Acc. Chem. Res.* **1987**, *20*, 301. (b) Bernasconi, C. F. *Adv. Phys. Org. Chem.* **1992**, *27*, 119. (c) Bernasconi, C. F. *Acc. Chem. Res.* **1992**, *25*, 9. (d) Bernasconi, C. F. *Adv. Phys. Org. Chem.* **2010**, *44*, 223.

(5) (a) A reactant stabilizing factor that is lost ahead of bond changes increases the intrinsic barrier while a reactant stabilizing factor whose loss lags behind bond changes lowers the intrinsic barrier. (b) For reactant and product *de*stabilizing factors all the above relations are reversed, e.g., a product destabilizing factor that lags behind bond changes lowers the intrinsic barrier, etc.

(6) (a) Bernasconi, C. F.; Sun, W.; García-Río, L.; Kin-Yan; Kittredge, K. *J. Am. Chem. Soc.* **1997**, *119*, 5583. (b) Bernasconi, C. F.; Kittredge, K. W. *J. Org. Chem.* **1998**, *63*, 1944. (c) Bernasconi, C. F.; Ali, M. *J. Am. Chem. Soc.* **1999**, *121*, 3039. (d) Bernasconi, C. F.; Sun, W. *J. Am. Chem. Soc.* **2002**, *124*, 2799. (e) Bernasconi, C. F.; Ali, M.; Gunter, J. C. *J. Am. Chem. Soc.* **2003**, *125*, 151. (f) Bernasconi, C. F.; Fairchild, D. E.; Montañez, R. L.; Aleshi, P.; Zheng, H.; Lorance, E. *J. Org. Chem.* **2005**, *70*, 7721. (g) Bernasconi, C. F.; Ragains, M. L. *J. Organomet. Chem.* **2005**, *690*, 5616. (h) Bernasconi, C. F.; Pérez-Lorenzo, M.; Brown, S. D. *J. Org. Chem.* **2007**, *72*, 4416.

(7) (a) Terrier, F.; Lelièvre, J.; Chatrousse, A.-P.; Farrell, P. *J. Chem. Soc., Perkin Trans. 2* **1985**, 1479. (b) Terrier, F.; Xie, H.-Q.; Lelièvre, J.; Boubaker, T.; Farrell, P. G. *J. Chem. Soc., Perkin Trans. 2* **1990**, 1899. (c) Moutiers, G.; El Fahid, B.; Collet, A.-G.; Terrier, F. *J. Chem. Soc., Perkin Trans. 2* **1996**, 49. (d) Moutiers, G.; El Fahid, B.; Goumont, R.; Chatrousse, A.-P.; Terrier, F. *J. Org. Chem.* **1996**, *61*, 1978.

(8) (a) Nevy, J. B.; Hawkinson, D. C.; Blotny, G.; Yao, X.; Pollack, R. M. *J. Am. Chem. Soc.* **1997**, *119*, 12722. (b) Yao, X.; Gold, M.; Pollack., R. M. *J. Am. Chem. Soc.* **1999**, *121*, 6220.

(9) Zhong, Z.; Snowden, T. S.; Best, M. D.; Anslyn, E. V. *J. Am. Chem. Soc.* **2004**, *126*, 3488.

(10) Kresge, A. J. *Can. J. Chem.* **1974**, *52*, 1897.

(11) For earlier important work on solvation, see refs 12 and 13.

(12) Cox, B. G.; Gibson, A. *Chem. Soc., Faraday Symp.* **1975**, *10*, 107.

(13) Keeffe, J. R.; Morey, J.; Palmer, C. A.; Lee, J. C. *J. Am. Chem. Soc.* **1978**, *101*, 1295.

(14) Polarizability effects drop off with the fourth power of distance while inductive effects drop off with square of distance.[15]

(15) Taft, R. W.; Topsom, R. D. *Prog. Phys. Org. Chem.* **1987**, *119*, 7545.

(16) (a) Bernasconi, C. F.; Ragains, M. L.; Bhattacharya, S. *J. Am. Chem. Soc.* **2003**, *125*, 12328. (b) Bernasconi, C. F.; Pérez-Lorénzo, M. *J. Am. Chem. Soc.* **2007**, *129*, 2704.

(17) (a) Bernasconi, C. F.; Wenzel, P. J.; Ragains, M. L. *J. Am. Chem. Soc.* **2008**, *130*, 4934. (b) Bernasconi, C. F.; Yamataka, H.; Yoshimura, N.; Sato, M. *J. Org. Chem.* **2009**, *74*, 188.

reference systems (reactions 3b and 4b), a reduction in the intrinsic barrier of 11 kcal/mol due to the aromaticity effect was calculated for reaction 3a and of 7.6 kcal/mol for reaction 4a. The larger reduction for reaction 3a is consistent with the greater aromatic stabilization energy (ASE) of benzene (36.3 kcal/mol) compared to that of cyclopentadienyl anion (29.4 kcal/mol).[17a]

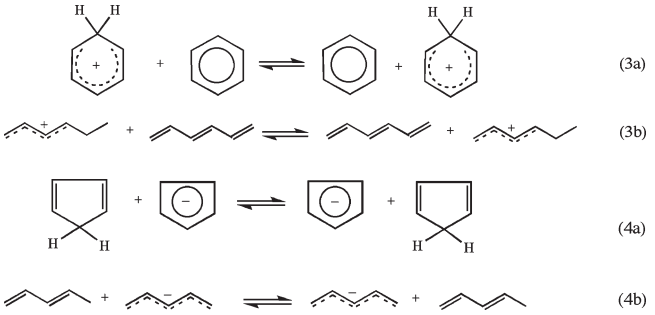

An important additional finding from the above study was that the development of aromaticity and that of charge delocalization at the transition state are decoupled. This means charge delocalization still lags behind proton transfer as is the case in nonaromatic systems and hence should increase the intrinsic barrier. This increase is not observable in reactions 3a and 4a because it is more than offset by the barrier reduction arising from the aromaticity. However, there may be systems where the aromaticity effect is considerably smaller than for reactions 3a or 4a and hence may not be able to compensate for the intrinsic barrier enhancing delocalization effect.

In this paper we propose to examine in more detail the relationship between aromatic stabilization energies and the effect on intrinsic barriers. To this end we have performed calculations on the identity proton transfers in the aromatic heterocyclic systems of reaction 5a as well as the corresponding noncyclic reference systems of reaction 5b.

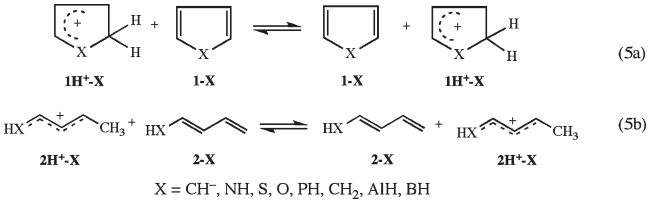

There have been numerous reports of aromatic stabilization energies of aromatic heterocycles in the literature. Following Cyránski's review[18] the aromaticity of **1-X** follows the order **1-CH**$^-$ (−22.1) > **1-NH** (−20.6) > **1-S** (−18.6) > **1-O** (−14.8) > **1-PH** (−3.2) > **1-CH$_2$** (0.0) > **1-AlH** (10.0) > **1-BH** (22.5) with the numbers being the ASEs in kcal/mol; **1-CH$_2$** is nonaromatic, and **1-AlH** and **1-BH** are antiaromatic. The low aromaticity of **1-PH** is due to the nonplanarity of phosphole, a feature to which we will return below.

Results and Discussion

In keeping with our previous work,[17a] all of our calculations were performed at the MP2/6-311+G** level of theory. The computational data are summarized in Tables S1−S74 of the Supporting Information.[19]

(18) Cyránski, M. K. *Chem. Rev.* **2005**, *105*, 3773.

Geometries. Bond lengths of the various structures described in reactions 5a and 5b as well as of the transition states of the respective reactions are shown in Chart 1. Bond angles, dihedral angles, and pyramidal angles are reported in Tables S76−S81 and Figures S1−S9 in Supporting Information;[19] the pyramidal angles, α, are defined as illustrated for the conjugate acid (**3**) and the transition state (**4**).

Those geometric parameters that are of particular interest are summarized in Table 1. The following points are noteworthy:

1. The structures of **1-X** are planar for X = CH$^-$, NH, S, O, BH, AlH, and CH$_2$ as indicated by the dihedral angle *d*(xccc) of zero or very close to zero, whereas **1-X** with X = PH is slightly puckered, with *d*(xccc) = 8.80°. Similar *d*(xccc) values have been reported for **1-PH** in previous studies.[20,21] An even larger dihedral angle (18.4°) is observed for **1H$^+$-PH**. For **1-PH** we have also calculated a structure constrained to have a planar geometry. As discussed below, this planar phosphole is much more aromatic than the optimized structure.

2. The C−C bond lengths, r_{cc1} and r_{cc2}, in **1-X** (Chart 1) show a pattern that reflects the aromaticity of **1-X** (X = CH$^-$, NH, S, O, PH) as well as the nonaromaticity or antiaromaticity of **1-X** (X = CH$_2$, BH, AlH). Specifically, for the latter group, r_{cc1} ranges from 1.355 to 1.361 Å while r_{cc2} ranges from 1.468 to 1.516 Å, which indicates strong double bond character for r_{cc1} and strong single bond character for r_{cc2}.[22] For the aromatic systems r_{cc1} ranges from 1.368 to 1.420 while r_{cc2} ranges from 1.420 to 1.432. The larger r_{cc1} and smaller r_{cc2} values in the aromatic systems are consistent with the contribution of the resonance structures **a**−**d**. We also note that r_{cc1} = 1.410 Å for the planar phosphole is considerably longer than for the optimized (1.368 Å), consistent with a greater contribution of **a**−**d** to its structure.

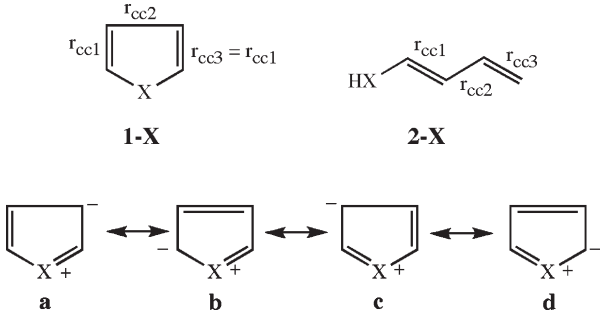

For **2-X** where aromaticity or antiaromaticity plays no role, one would expect minimal variations in the r_{cc1}, r_{cc2}, and r_{cc3} values (Table 2). In fact, except for **2-CH**$^-$, the r_{cc1}

(19) See paragraph concerning Supporting Information at the end of this article.
(20) Chesnut, D. B.; Quin, L. D. *Heteroatom. Chem.* **2004**, *18*, 754.
(21) Vessaly, B. *J. Struct. Chem.* **2008**, *49*, 979.
(22) C(sp^2)−C(sp^2) single bonds typically range from 1.45 to 1.48 Å while C=C double bonds typically range from 1.31 to 1.34 Å.[23]

CHART 1

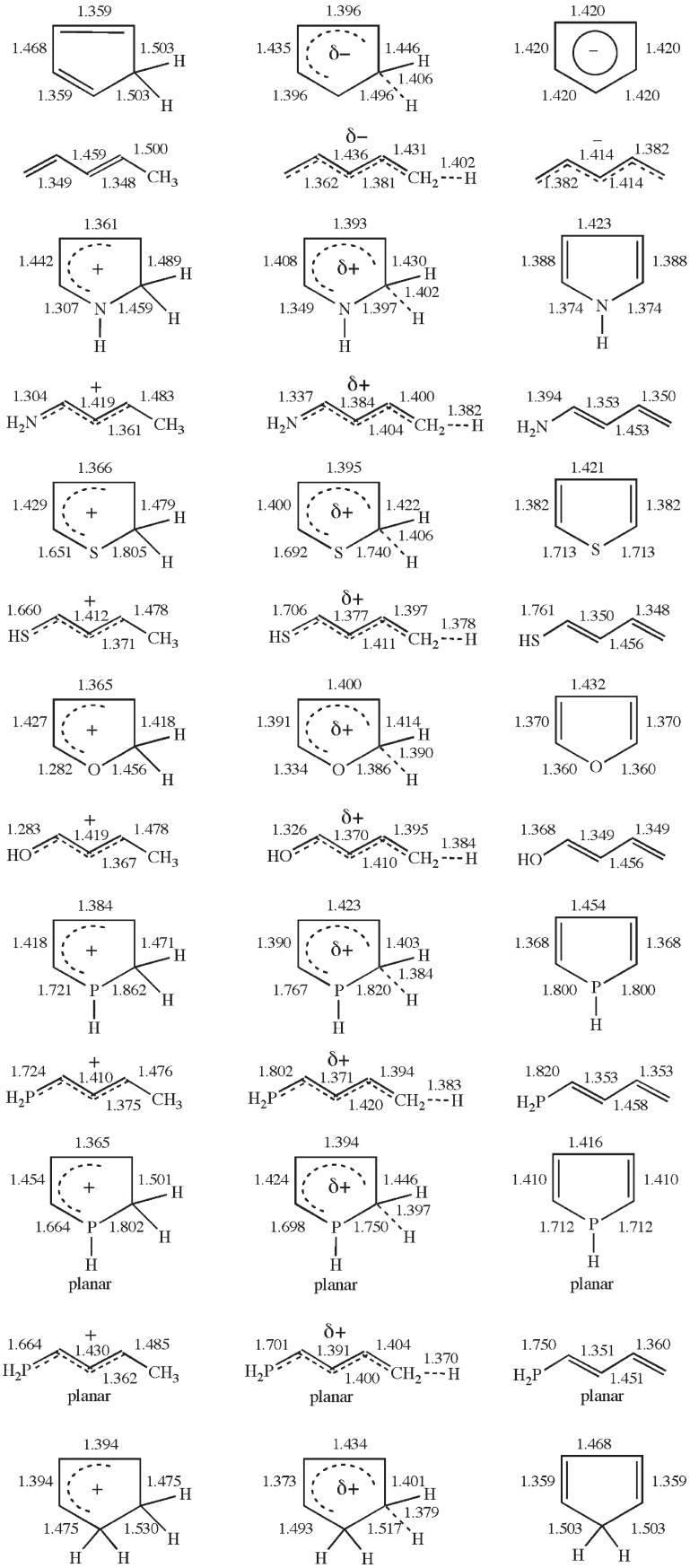
1.359
1.468
1.503
H
1.359
1.503
H
1.396
δ−
1.435
1.446
H
1.406
1.396
1.496
H
1.420
−
1.420
1.420
1.420
1.420
1.459
1.500
1.349
1.348
CH3
δ−
1.436
1.431
1.402
1.362
1.381
CH2
H
1.414
1.382
1.382
1.414
1.361
+
1.442
1.489
H
1.307
N
1.459
H
H
1.393
δ+
1.408
1.430
H
1.402
1.349
N
1.397
H
H
1.423
1.388
1.388
1.374
N
1.374
H
+
1.304
1.419
1.483
H2N
1.361
CH3
δ+
1.337
1.384
1.400
1.382
H2N
1.404
CH2
H
1.394
1.353
1.350
H2N
1.453
1.366
+
1.429
1.479
H
1.651
S
1.805
H
1.395
δ+
1.400
1.422
H
1.406
1.692
S
1.740
H
1.421
1.382
1.382
1.713
S
1.713
+
1.660
1.412
1.478
HS
1.371
CH3
δ+
1.706
1.377
1.397
1.378
HS
1.411
CH2
H
1.761
1.350
1.348
HS
1.456
1.365
+
1.427
1.418
H
1.282
O
1.456
H
1.400
δ+
1.391
1.414
H
1.390
1.334
O
1.386
H
1.432
1.370
1.370
1.360
O
1.360
+
1.283
1.419
1.478
HO
1.367
CH3
δ+
1.326
1.370
1.395
1.384
HO
1.410
CH2
H
1.368
1.349
1.349
HO
1.456
1.384
+
1.418
1.471
H
1.721
P
1.862
H
H
1.423
δ+
1.390
1.403
H
1.384
1.767
P
1.820
H
H
1.454
1.368
1.368
1.800
P
1.800
H
+
1.724
1.410
1.476
H2P
1.375
CH3
δ+
1.802
1.371
1.394
1.383
H2P
1.420
CH2
H
1.820
1.353
1.353
H2P
1.458
1.365
+
1.454
1.501
H
1.664
P
1.802
H
H
planar
1.394
δ+
1.424
1.446
H
1.397
1.698
P
1.750
H
H
planar
1.416
1.410
1.410
1.712
P
1.712
H
planar
+
1.664
1.430
1.485
H2P
1.362
CH3
planar
δ+
1.701
1.391
1.404
1.370
H2P
1.400
CH2
H
planar
1.750
1.351
1.360
H2P
1.451
planar
1.394
+
1.394
1.475
H
1.475
1.530
H
H
H
1.434
δ+
1.373
1.401
H
1.379
1.493
1.517
H
H
H
1.468
1.359
1.359
1.503
1.503
H
H

CHART 1. Continued

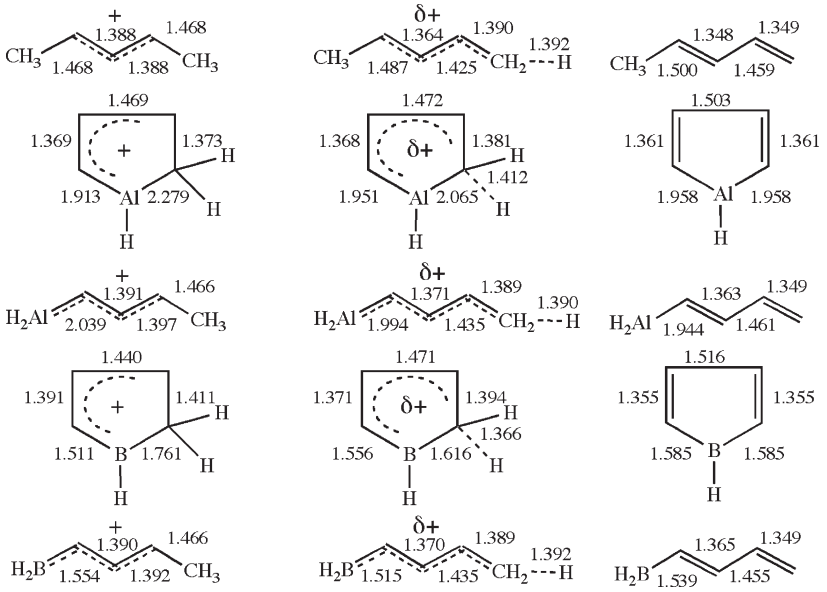

TABLE 1. Selected Geometric Parameters (Reaction 5a)[a]

	r_{cc1}			r_{cc2}			r_{cc3}[e]		d(xccc)[b]	α[c]			C−H−C[d]	
X	**1H$^+$-X**	TS	**1-X**	**1H$^+$-X**	TS	**1-X**	**1H$^+$-X**	TS	**1-X**	**1H$^+$-X**	TS	**1-X**	cyclic systems	linear systems
CH^-	1.468	1.435	1.420	1.359	1.396	1.420	1.503	1.446	0.000	53.47	21.90	0.00	1.406	1.402
NH	1.442	1.408	1.388	1.361	1.393	1.423	1.489	1.430	0.000	54.89	27.56	0.00	1.402	1.382
S	1.429	1.400	1.382	1.366	1.395	1.421	1.479	1.422	0.000	53.38	26.56	0.00	1.406	1.378
O	1.427	1.391	1.370	1.365	1.400	1.432	1.479	1.414	0.040	55.32	29.31	0.00	1.390	1.384
PH	1.418	1.390	1.368	1.384	1.423	1.454	1.471	1.403	8.800	60.2	32.31	0.00[f]	1.384	1.383
PH (planar)	1.454	1.424	1.410	1.365	1.394	1.416	1.501	1.446	0.000	55.9	30.99	0.00	1.397	1.370
CH_2	1.394	1.373	1.359	1.394	1.434	1.468	1.475	1.401	0.000	52.79	25.82	53.47	1.379	1.392
AlH	1.369	1.368	1.361	1.469	1.472	1.516	1.373	1.384	−0.005	60.2	28.84	0.00	1.412	1.390
BH	1.391	1.371	1.355	1.440	1.471	1.503	1.411	1.394	0.005	50.77	34.50	0.00	1.366	1.392

[a]Bond lengths in Å. [b]Dihedral angle. [c]Pyramidal angle. [d]C−H bond length at the transition state. [e]For **1-X** $r_{cc3} = r_{cc1}$ [f]Pyramidal angle at phosphorus is 73.3°.

TABLE 2. Selected Bond Lengths (Reaction 5b)[a]

	r_{cc1}			r_{cc2}			r_{cc3}		
X	**2H$^+$-X**	TS	**2-X**	**2H$^+$-X**	TS	**2-X**	**2H$^+$-X**	TS	**2-X**
CH^-	1.459	1.436	1.414	1.348	1.381	1.414	1.500	1.431	1.382
NH	1.419	1.384	1.353	1.361	1.404	1.453	1.483	1.400	1.350
S	1.412	1.377	1.350	1.371	1.411	1.456	1.478	1.397	1.348
O	1.419	1.370	1.349	1.367	1.410	1.456	1.478	1.395	1.348
PH	1.410	1.371	1.353	1.375	1.420	1.458	1.476	1.394	1.353
PH (planar)	1.430	1.391	1.360	1.362	1.400	1.451	1.485	1.404	1.359
CH_2	1.388	1.364	1.348	1.388	1.425	1.500	1.468	1.390	1.349
AlH	1.391	1.371	1.363	1.397	1.435	1.461	1.466	1.389	1.349
BH	1.390	1.370	1.365	1.392	1.435	1.455	1.466	1.389	1.349

[a]Bond lengths in Å.

values range from 1.348 to 1.365 Å, r_{cc2} ranges from 1.453 to 1.461 Å, and r_{cc3} ranges from 1.348 to 1.353 Å, i.e., r_{cc1} and r_{cc3} are close to the values for double bonds[22] while r_{cc2} is close to the value for single bonds.[22] **2-CH$^-$** is different in that it is a fully delocalized and symmetrical anion with $r_{cc1} = r_{cc2} = 1.414$ Å, a value approximately halfway between that for a single and a double bond,[22] and $r_{cc3} = 1.382$ Å, which is closer to that for a double bond, consistent with the three main resonance structures of this anion.

3. In **1H$^+$-X** r_{cc1} and r_{cc2} (Table 1) reveal a pattern that reflects the π-donor strength of X. For **1H$^+$-X** (X = CH^-, NH, S, O, PH) r_{cc1} tends to be longer (1.418−1.468 Å) and r_{cc2} tends to be shorter (1.361−1.384 Å) than for **1H$^+$-X** (X = CH_2, BH, AlH), where r_{cc1} ranges from 1.354 to 1.391 Å and r_{cc2} ranges from 1.394 to 1.469 Å. This is consistent with the increasing contribution of the resonance structure **g**, which tends to lengthen r_{cc1} and shorten r_{cc2}. With the strongest π-donors (X = CH^-, NH, S, O, PH (planar)), r_{cc1} is the longest and r_{cc2} is the shortest. For **1H$^+$-X** (X = CH_2, BH, AlH) there is no contribution by **g** and hence r_{cc1} is short and r_{cc2} long. The r_{cc3} values for all **1H$^+$-X** except

(23) Anslyn, E. V.; Dougherty, D. A. *Modern Physical Organic Chemistry*; University Science Books: Sausalito, CA, 2006; p 22.

TABLE 3. Changes in r_{cc1}, r_{cc2} and r_{cc3} During Reaction 5a,[a]

	Δr_{cc1}			Δr_{cc2}			Δr_{cc3}		
X	**1H$^+$-X** → TS	**1H$^+$-X** → **1-X**	% at TS[b]	**1H$^+$-X** → TS	**1H$^+$-X** → **1-X**	% at TS[b]	**1H$^+$-X** → TS	**1H$^+$-X** → **1-X**	% at TS[b]
CH^-	−0.033	−0.048	68.8	0.037	0.061	64.1	−0.057	−0.083	68.7
NH	−0.034	−0.054	63.0	0.032	0.062	51.6	−0.059	−0.101	58.4
S	−0.029	−0.047	61.7	0.029	0.055	52.3	−0.057	−0.097	58.4
O	−0.036	−0.057	63.2	0.035	0.067	52.2	−0.065	−0.109	59.6
PH	−0.028	−0.050	56.0	0.039	0.070	55.7	−0.068	−0.103	66.0
PH (planar)	−0.030	−0.044	68.2	0.029	0.051	56.9	−0.055	−0.091	60.4
CH_2	−0.021	−0.035	60.0	0.040	0.074	54.1	−0.077	−0.119	60.4
AlH	−0.001	−0.008	12.5	0.003	0.047	6.4	0.008	−0.012	
BH	−0.020	−0.036	55.5	0.031	0.063	49.2	−0.017	−0.056	30.4

[a]Bond lengths in Å. [b]Percent change at the transition state.

1H$^+$-AlH and **1H$^+$-BH** range from 1.471 to 1.503 Å, which is typical for C−C single bonds as one would expect. For **1H$^+$-BH** and especially for **1H$^+$-AlH** r_{cc3} is unusually short (1.373 and 1.411 Å, respectively). The distortions suggested by these short r_{cc3} values are associated with unusually long Al−C(sp^3) (2.279 Å)[24] and B−C(sp^3) (1.761 Å) bonds.[26]

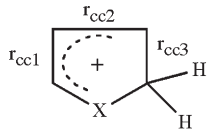

1H$^+$-X

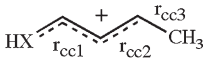

2H$^+$-X

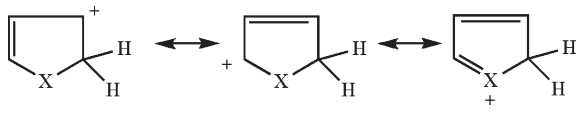

e **f** **g**

As revealed in Table 2, the patterns for r_{cc1} and r_{cc2} in **2H$^+$-X** are quite similar to those in **1H$^+$-X**, i.e., larger r_{cc1} and smaller r_{cc2} values when X is a π-donor (X = CH^-, NH, S, O, PH). This reflects the contribution of the resonance structure **j**. The r_{cc3} values range from 1.466 to 1.483 Å for all **2H$^+$-X** except for **2H$^+$-CH$^-$**, reflecting essentially single bond character. The somewhat longer r_{cc3} (1.500 Å) for **2H$^+$-CH$^-$** may be attributed to the fact that this is not a cation and hence there is no hyperconjugation (**k**) that may have a r_{cc3} shortening effect.

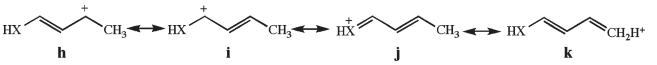

h **i** **j** **k**

4. Table 3 reports the *changes* in r_{cc1}, r_{cc2}, and r_{cc3} along the reaction coordinate for the heterocyclic systems. For the aromatic systems the % changes at the transition state tend to be > 50% and somewhat higher than for the nonaromatic or antiaromatic systems; the unusually low % changes for the **1H$^+$-AlH**/**1-AlH** system probably reflect the structural anomalies of **1H$^+$-AlH** mentioned above. The higher % changes for the aromatic systems imply that for the latter systems the two fragments of the transition state are structurally more similar to **1-X** than to **1H$^+$-X**. Even though consistent with other measures of transition structures discussed below that suggest that the development of aromaticity is ahead of proton transfer, there may not be a causal connection if systems such as reaction 6 can offer any guidance. In these systems charge delocalization/resonance stabilization not only do not track bond changes but actually lag behind such changes, and it was shown that tracking should actually not be expected.[28] Hence there may be no direct connection between aromaticity and bond changes in reactions 5a either, a conclusion reenforced by the results for the linear reference systems (reaction 5b) summarized in Table 4. Specifically, the percent changes reported in Table 4 indicate that at the transition state the r_{cc1} and r_{cc3} values are much closer to those for **2-X** than to **2H$^+$-X** while the r_{cc2} values are closer to the midpoint between **2H$^+$-X** and **2-X**. As discussed below, this contrasts with the degree of charge delocalization that lags behind proton transfer at the transition state. The unusually low Δr_{cc3} values as well as the low percent change in r_{cc3} for the **2-CH$^-$** system appears to be related to absence of hyperconjugation (**k**) in **2H$^+$-CH** that renders r_{cc3} larger than for the other systems.

$$Y-CH_3 + CH_2{=}Y^- \rightleftharpoons Y{=}CH_2 + CH_3-Y \qquad (6)$$

5. For all reactions 5a and 5b, the two fragments of the transition state are in an anti relationship and the C−H−C angle is 180° as is the case for reactions 3a and 3b.[17a] The C−H−C bonds (Table 1) at the transition state for the reactions of the aromatic systems (X = CH^-, NH, S, O, PH) range from 1.384 to 1.406 Å; within this group there is a trend toward longer bonds with increasing aromaticity. For the antiaromatic **1-BH** system these bonds are much shorter (1.366 Å), for the nonaromatic **1-CH$_2$** system they are between the above ranges (1.379 Å), and for the antiaromatic **1-AlH** system they are unusually long (1.412 Å). For the reactions 5b where aromaticity/antiaromaticity does not come into play, most C−H−C bond lengths are in a very narrow range (1.382−1.392 Å) except for the **2-CH$_2$** system where they are 1.402 Å and for the **2-PH**(planar) system (1.370 Å).

The dependence of the C−H−C bond lengths on aromaticity may reflect a delicate balance between stabilizing and destabilizing factors. The former may include the aromatic character of the transition state and the tightness of the C−H−C bonds while the latter is the steric repulsion of the two fragments. For the highly aromatic transition states there is less need for additional stabilization by tight C−H−C bonds which allows the two fragments to be farther apart thereby reducing steric repulsion; the longer bonds also enhance the aromaticity of the transition state. On the other hand, in the absence of aromatic stabilization, and even more so for the antiaromatic **1-BH** system, C−H−C bond tightness becomes a dominant source of stabilization despite

(24) The Al−C bond in $(CH_3)_3Al$ is 1.957 Å.[25]
(25) Almenningen, A.; Halvorsen, S.; Haaland, A. *Acta Chem. Scand.* **1971**, *25*, 1937.
(26) The B−C bond in trimethyl borane is 1.560 Å.[27]
(27) Lévy, H. A.; Brockway, L. O. *J. Am. Chem. Soc.* **1937**, *59*, 2085.
(28) Bernasconi, C. F.; Wenzel, P. J. *J. Am. Chem. Soc.* **1994**, *116*, 5405.

TABLE 4. Changes in r_{cc1}, r_{cc2}, and r_{cc3} During Reaction 5b,[a]

	Δr_{cc1}			Δr_{cc2}			Δr_{cc3}		
X	**2H$^+$-X** → TS	**2H$^+$-X** → **2-X**	% at TS[b]	**2H$^+$-X** → TS	**2H$^+$-X** → **2-X**	% at TS[b]	**2H$^+$-X** → TS	**2H$^+$-X** → **2-X**	% at TS[b]
CH$^-$	−0.064	−0.086	74.4	0.033	0.066	50.0	−0.028	−0.067	41.8
NH	−0.035	−0.066	53.0	0.043	0.092	46.7	−0.083	−0.133	62.4
S	−0.035	−0.062	56.4	0.040	0.085	47.0	−0.081	−0.130	62.3
O	−0.049	−0.070	70.0	0.043	0.089	48.3	−0.083	−0.129	69.7
PH	−0.039	−0.057	68.4	0.045	0.083	54.2	−0.082	−0.123	66.7
PH (planar)	−0.039	−0.070	55.7	0.038	0.089	42.7	−0.081	−0.126	64.3
CH_2	−0.024	−0.040	60.0	0.037	0.112	33.0	−0.078	−0.119	65.5
AlH	−0.020	−0.028	71.4	0.038	0.064	55.4	−0.077	−0.117	65.8
BH	−0.020	−0.025	80.0	0.043	0.063	68.3	−0.077	−0.117	65.8

[a]Bond lengths in Å. [b]Percent change at the transition state.

TABLE 5. NICS(1) Values

X	**1H$^+$-X**	TS	**1-X** (lit.)[a]	% change[b]
CH$^-$	−5.1	−8.3	−9.4 (−10.3)	74.4
NH	−6.3	−9.2	−10.4 (−10.6)	70.7
S	−7.5	−10.2	−10.9 (−10.8)	78.5
O	−7.0	−9.2	−9.9 (−9.4)	75.9
PH	−5.6	−8.8	−6.8 (−6.0)	> 100
PH (planar)	−6.1	−10.9	−11.2 (−17.4)[c]	93.2
AlH	−5.6	−5.2	3.0 (3.1)	4.7
BH	−4.5	−0.6	10.3 (9.2)	26.4

[a]Reference 18. [b][NICS(TS) − NICS(**1H$^+$-X**)]/[NICS(**1-X**) − NICS(**1H$^+$-X**)] × 100. [c]NICS(0), ref 31.

increased steric repulsion. Only for the **1-AlH** system the steric repulsion is so strong as to become the overriding factor that leads to the very long C−H−C bonds.

NICS(1) Values as Measures of Aromaticity. Table 5 summarizes NICS(1) values[29,30] for **1H$^+$-X**, **1-X**, and the respective transition states of reactions 5a. The table also includes NICS(1) values for **1-X** reported by Cyránski[18] at the GIAO/HF/6-311+G**//MP2(fc)/6-311+G** level. There is good agreement between Cyránski's and our values; the small differences must be the result of the different levels of theory used in the two laboratories.

The most interesting and important findings from these calculations refer to the changes in the NICS(1) values that result when moving along the reaction coordinate, in particular the % change of these values that has occurred at the transition state. For all of the aromatic systems (X = CH$^-$, NH, S, O, PH (planar)), this change is well above 50%. Since because of the symmetry of reaction 5a the progress of proton transfer at the transition state is exactly 50%, our results imply that the development of aromaticity at the transition state is significantly ahead of proton transfer just as was found to be the case for reaction 3a[17a] and reaction 7 (X = O and S).[17b]

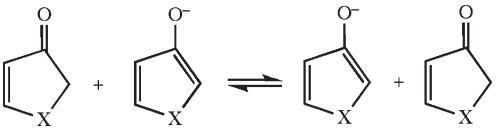

(7)

The % change above 100% for X = PH, which implies that the transition state is more aromatic than **1-PH**, may represent an artifact resulting from the nonplanarity of **1H$^+$-PH** (d(xccc) = 18.4°). The consequence of this nonplanarity is that the phosphorus lone pair may be able to exert a slight anomeric effect. There are three observations that support such an interpretation:

1. The C−H bond lengths on the carbon adjacent to the phosphorus atom are unequal as shown in **5**.

2. The progress in the shortening of the P−C bond at the transition state of the conversion of **1H$^+$-PH** to **1-PH** is 67%, which is significantly higher than the 45.6% progress of the same bond shortening in the conversion of **1H$^+$-PH**-(planar) to **1-PH**(planar).[31] This is consistent with participation of the phosphorus lone pair in expelling the proton (anchimeric assistance), thereby contributing to the build-up of aromaticity (**6**). Note that once the proton has left, the anomeric effect disappears and with it its potential contribution to enhanced aromaticity.

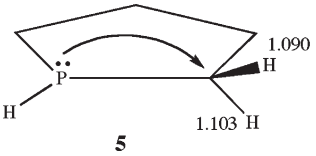

5

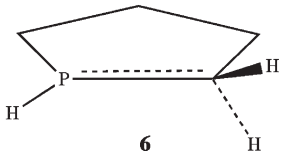

6

3. As discussed below, the reaction barrier ($\Delta H^{\ddagger}$) for the **1H$^+$-PH**/**1-PH** system is lower than one would anticipate on the basis of the ASE of **1-PH**, which is consistent with transition state stabilization by the anomeric effect. We also note that if the positions of the phosphorus lone pair and phosphorus hydrogen are switched so as to preclude an anomeric effect, the transition state energy is raised by 8.4 kcal/mol.

For the two antiaromatic systems (X = AlH, BH), the low percent changes in the NICS(1) values imply that the development of antiaromaticity at the transition state lags behind proton transfer, again consistent with an earlier finding for reaction 8 involving the antiaromatic cyclobutadiene system.[17a]

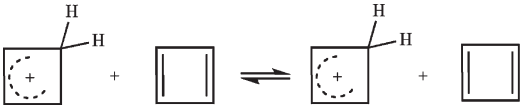

(8)

Charges and Charge Imbalance. Group charges for all species in reactions 5a and 5b calculated on the basis of NPA atomic charges are reported in Chart 2. As has been observed in reactions 3a, 3b, 4a, and 4b, as well as 6 and 8, the proton-in-flight at the transition state carries a significant amount of positive charge. For the cyclic systems these positive charges range from 0.302 to 0.376 with the exception of the **1H$^+$-AH**/**1-AlH** system where it is 0.251; for the linear systems they range from 0.276 to 0.315.

(29) (a) Schleyer, P. v. R.; Maerker, C.; Dransfeld, A.; Jiao, H.; van Eikema Hommes, W. J. R. *J. Am. Chem. Soc.* **1996**, *118*, 6317. (b) Chen, Z.; Wannese, C. S.; Corminboeuf, C.; Puenta, R.; Schleyer, P. v. R. *Chem. Rev.* **2005**, *105*, 3342.

(30) NICS(1) values determined 1 Å above the ring center have recently been recognized as being a more reliable measures of aromaticity compared to NICS(0) evaluated at the center.[29b]

CHART 2

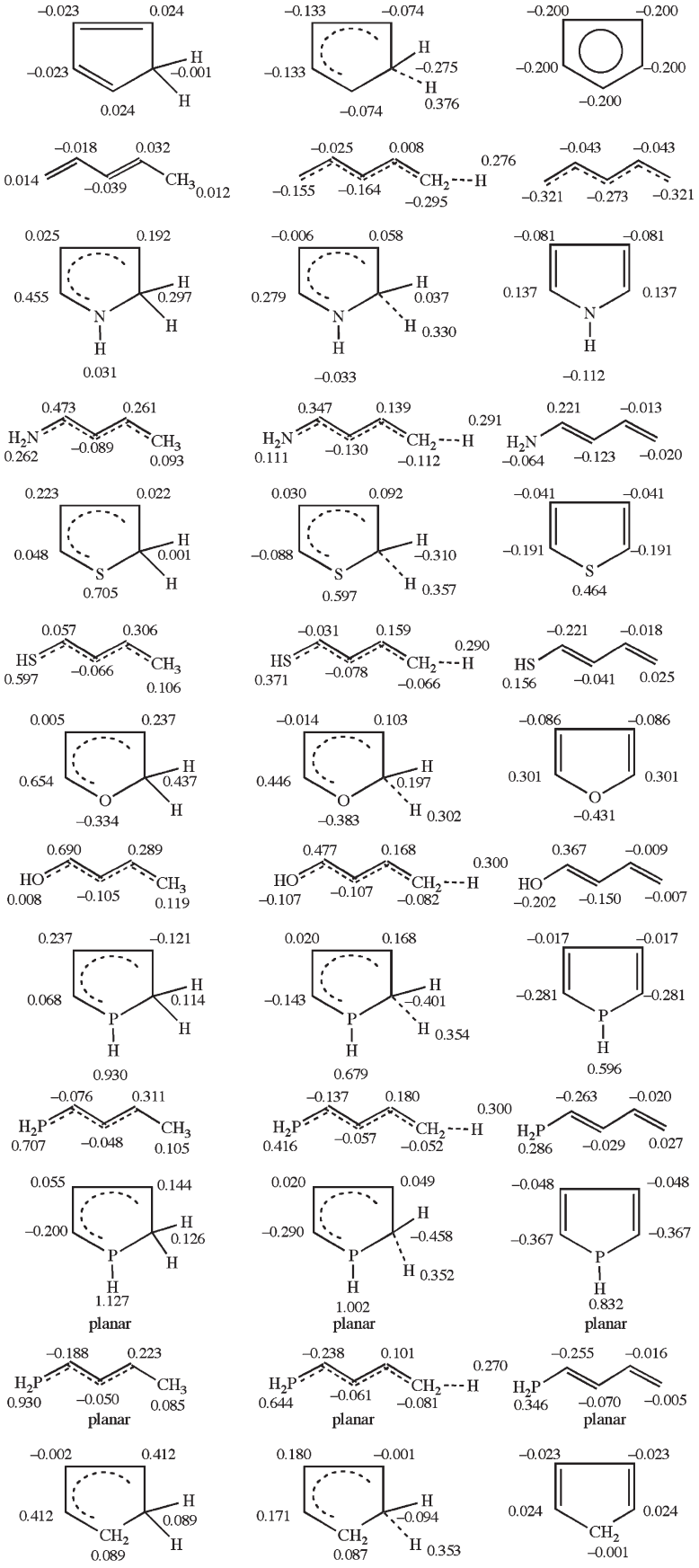

CHART 2. Continued

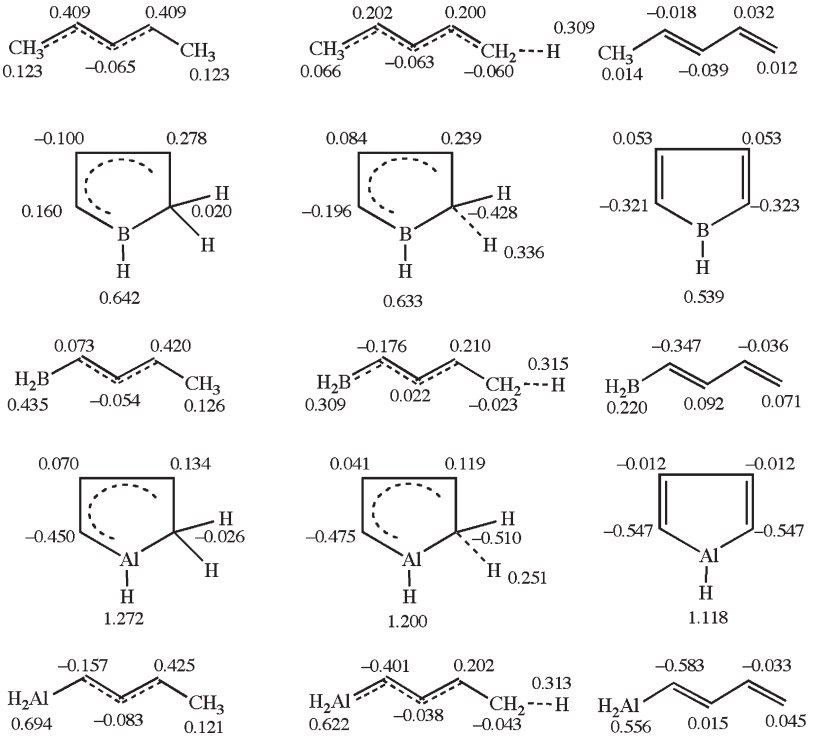

TABLE 6. Proton Affinities, Intrinsic Barriers, and Aromatic Stabilization Energies[a]

system	$\Delta H°$	$\Delta\Delta H°$[b]	$\Delta H^{‡}$ (298 K)	$\Delta H^{‡}_{corr}$ (298 K)[c]	$\Delta\Delta H^{‡}_{corr}$ (298 K)[d]	ASE[e]
1H$^+$-CH$^-$/1-CH$^-$	349.1	−24.9	−2.67	2.18	−7.41	−22.1
2H$^+$-CH$^-$/2-CH$^-$	374.0		6.41	9.59		
1H$^+$-NH/1-NH	203.5	−23.4	−3.64	0.15	−5.60	−20.6
2H$^+$-NH/2-NH	226.9		3.07	5.75		
1H$^+$-S/1-S	190.7	−16.7	−5.38	−0.09	−5.43	−18.6
2H$^+$-S/2-S	207.4		2.43	5.34		
1H$^+$-O/1-O	189.7	−12.3	−1.00	2.78	3.30	−14.8
2H$^+$-O/2-O	202.0		−3.25	−0.52		
1H$^+$-PH/1-PH	194.5	−5.2	3.55	9.01	3.77	−3.2
2H$^+$-PH/2-PH	199.7		2.45	5.24		
1H$^+$-PH/1-PH (planar)	204.8	−22.6	−10.85	−4.85	−13.4	−26.0[f]
2H$^+$-PH/2-PH (planar)	227.4		5.56	8.55		
1H$^+$-CH$_2$/1-CH$_2$	193.8	−3.7	−6.78	−2.19	−2.85	0.0
2H$^+$-CH$_2$/2-CH$_2$	197.5		−1.98	0.66		
1H$^+$-AlH/1-AlH	210.5	21.8	−2.03	5.87	4.80	10.0
2H$^+$-AlH/2-AlH	188.7		-1.68	1.07		
1H$^+$-BH/1-BH	195.6	10.7	−5.02	−1.61	−8.63	22.5
2H$^+$-BH/2-BH	184.9		4.41	7.02		

[a]In kcal/mol. [b]$\Delta\Delta H° = \Delta H°$(**1-X**) − $\Delta H°$(**2-X**). [c]Corrected for BSSE. [d]$\Delta\Delta H^{‡}_{corr} = \Delta H^{‡}_{corr}$(**1-X**) − $\Delta H^{‡}_{corr}$(**2-X**). [e]ASE = aromatic stabilization energies taken from ref 18. [f]Reference 36 (B3LYP/6-311+G**).

One of the most significant conclusions that can be derived from the charges is that, upon conversion of **1H$^+$-X** to **1-X**, charge delocalization lags behind proton transfer. This is seen from the large decrease (from strongly to weakly positive, or from weakly positive to negative, or from negative to strongly negative) in the charge on the reaction site as **1H$^+$-X** reaches the transition state, which is followed by an increase (from positive to more positive, or from negative to positive, or from negative to less negative) as the transition state collapses into **1-X**. In other words, the negative charge being initially transferred to the reactive carbon at the transition state becomes partially delocalized in the product **1-X** in a similar way as in reactions 1 and 2. This is an important conclusion that confirms similar findings reported for reaction 3a,[17a] namely, that even in reactions where the development of aromaticity runs ahead of proton transfer, charge delocalization follows its usual pattern of late development,[4] i.e., the two processes are decoupled.

Other features related to the charge distributions summarized in Chart 2 will be discussed in the section about barriers.

Energies. A. General Considerations. Table 6 summarizes proton affinities ($\Delta H°$) and enthalpic barriers ($\Delta H^{‡}$) for reactions 5a and 5b for X = CH$^-$, NH, S, O, PH, PH (planar), CH$_2$, AlH, and BH calculated at the MP2/6-311+G** level of theory. A more detailed breakdown into electronic and zero

(31) The P−C bond lengths referred to are summarized in Figures S7 and S9 in Supporting Information.[19]

TABLE 7. Effects of Various Factors on the Stabilization of $1H^+$-X and 1-X and on $\Delta H°$[a]

factor	effect on stability of $1H^+$-X	effect on stability of 1-X	effect on $\Delta H°$
aromaticity		↑	↓
antiaromaticity		↓	↑
resonance	↑		↑
electron-withdrawing X	↓		↓
electron-donating X	↑		↑
polarizability of X	↑		↑
geometric distortion[b]	↓	↓	↑

[a]Arrows pointing up (down) mean stabilization (destabilization). [b]Destabilizing effect larger on **1-PH** than on $1H^+$-**PH**, see text.

point energies of all species involved is presented in Table S75 in Supporting Information.[19] For the barriers both uncorrected and BSSE[32]-corrected values are reported.

B. Proton Affinities. The major factors expected to affect the proton affinities of **1-X** and **2-X** are the electronic charge, aromaticity/antiaromaticity in the case of **1-X**, and the resonance stabilization of $1H^+$-**X** (in particular **g**) and $2H^+$-**X** (in particular **j**), respectively. Other more subtle factors include the inductive and polarizability effects of X and, in some cases such as **1-PH**(planar) and **1-AlH**, geometric distortion. Hence, the dependence of $\Delta H°$ on X is expected to be complex and not to simply follow the ASE values in the case of **1-X**. Nevertheless, the following points can be made.

1. Because $\Delta H°$ is defined as the enthalpy of reaction 9 (neutral base) or 10 (anionic base), respectively, $\Delta H°$ should be much higher for reaction 10 (charge separation) than for reaction 9. The large $\Delta H°$ values for **1-CH**$^-$ and **2-CH**$^-$ reflect this expectation.

$$BH^+ \rightarrow B + H^+ \quad (9)$$

$$BH \rightarrow B^- + H^+ \quad (10)$$

2. Regarding the dependence of $\Delta H°$ on X for the neutral **1-X**, factors that stabilize **1-X** (aromaticity) or destabilize $1H^+$-**X** (electron-withdrawing X) will decrease $\Delta H°$, whereas factors that destabilize **1-X** (antiaromaticity) or stabilize $1H^+$-**X** (electron-donating X, polarizability of X) will increase $\Delta H°$. The effect of these various factors are summarized in Table 7. The inductive and polarizability effects of X may be quite significant due to the proximity of X to the positive charge in resonance structure **f**. Geometric distortions destabilize both **1-X** and $1H^+$-**X**, and hence no prediction of the effect on $\Delta H°$ can be made although the data discussed below suggest a larger effect on **1-X** than on $1H^+$**X**, resulting in an increase in $\Delta H°$. Since none of the above-mentioned factors play a role for **1-CH$_2$**, we shall use its $\Delta H°$ (193.8 kcal/mol) as reference point in discussing the interplay of the various effects:
   - $\Delta H°$ for **1-S** (190.7 kcal/mol) is significantly lower than for **1-NH** (203.5 kcal/mol), indicating that the somewhat greater aromaticity of **1-NH** is overcompensated by the much stronger resonance stabilization of $1H^+$-**NH** compared to that of $1H^+$-**S**, rendering $\Delta H°$ for **1-NH$_2$** even higher than for **1-CH$_2$**.
   - $\Delta H°$ for **1-S** (190.7 kcal/mol) and **1-O** (189.7 kcal/mol) are almost the same because the stronger aromaticity of **1-S** is apparently offset by inductive and polarizability effects. Specifically, the stronger electron-withdrawing effect of O compared to S[34] destabilizes $1H^+$-**O** more than $1H^+$-**S** and hence lowers $\Delta H°$ of **1-O**[34] relative to that of **1-S**. The stronger polarizability of S stabilizes $1H^+$-**S** more than $1H^+$-**O**, which increases $\Delta H°$ for **1-S** relative to that of **1-O**.
   - The higher $\Delta H°$ for **1-PH** (194.5 kcal/mol) relative to that for **1-S** (190.7 kcal/mol) reflects mainly the lower aromaticity of the former, although small differences in the resonance, inductive, and polarizability effects of $1H^+$-**PH** versus $1H^+$-**S** probably affect the degree by which the proton affinities of the two compounds differ. Also note the fact that $\Delta H°$ for **1-PH** (194.5 kcal/mol) is slightly higher than for **1-CH$_2$** (193.8 kcal/mol), suggesting that the combined influence of the resonance and polarizability effects on $1H^+$-**PH** more than offset the aromaticity of **1-PH**.
   - The phosphole system constrained to be planar represents a particularly interesting situation. As was already shown by Dransfeld et al.,[36] **1-PH**-(planar) is much more aromatic than **1-PH** as indicated by a highly negative NICS value and other aromaticity indices. However, the higher aromaticity comes at the expense of increased strain resulting from the planarization of the phosphorus atom,[20,29] which leads to a net destabilization of the planar phosphole relative to **1-PH**. Our calculations indicate the destabilization is 15.9 kcal/mol, which compares with Chesnut and Quin's value of 18.2 kcal/mol (B3LYP/6-31+G**);[20] planarization of $1H^+$-**PH** destabilizes it by 5.6 kcal/mol. The result is $\Delta H°$ = 204.8 kcal/mol for **1-PH**(planar), which is 10.3 kcal/mol higher than for **1-PH**.
   - Because **1-BH** is antiaromatic, one expects a relatively high $\Delta H°$ and in fact its value, 195.6 kcal/mol, is higher than for **1-S**, **1-O**, and **1-PH**. However, it is only modestly higher than for the mentioned aromatic heterocycles, which may be mainly accounted for by the absence of a resonance effect in $1H^+$-**BH**.
   - $\Delta H°$ for **1-AlH** (210.5 kcal/mol) is the highest of all cyclic compounds studied. Since according to the ASEs **1-AlH** is less antiaromatic than **1-BH**, one would have expected $\Delta H°$ to be lower rather than higher than for **1-BH**. This unexpected result may be attributed to the structural anomalies of $1H^+$-**AlH** discussed in the section on geometries.
3. Because as discussed above so many other factors besides aromaticity/antiaromaticity affect the proton

(32) The BSSE (basis set superposition error) corrections were estimated by the counterpoise method.[33]

(33) Boys, S. F.; Bernardi, F. *Mol. Phys.* **1970**, *19*, 553.
(34) Using the MeO and MeS groups as a models, σ_F(OMe) = 0.30 and σ_F(SMe) = 0.20 for the inductive effect, σ_α(OMe) = −0.17 and σ_α(SMe) = −0.68 for the polarizability.[35]
(35) Hansch, C.; Leo, A.; Taft, R. W. *Chem. Rev.* **1991**, *91*, 165.
(36) Dransfeld, A.; Nyulászc, L.; Schleyer, P. v. R. *Inorg. Chem.* **1998**, *37*, 4413.

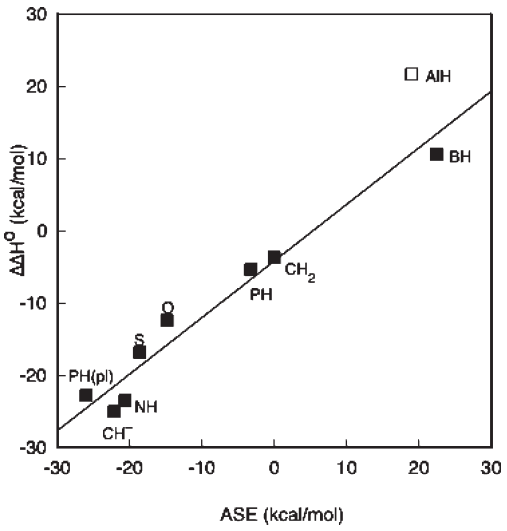

FIGURE 1. Plot of $\Delta\Delta H°$ versus ASE. Slope of line excluding the point for **1-AlH** is 0.747 ± 0.0067, intercept $= 4.53 \pm 1.22$ kcal/mol, $r = 0.977$.

affinities of **1-X**, it is difficult to evaluate the contribution of aromaticity/antiaromaticity to $\Delta H°$ of **1-X** in any quantitative way. However, $\Delta\Delta H°$, the difference between $\Delta H°$(**1-X**) and $\Delta H°$(**2-X**), which corresponds to the reaction enthalpy of reaction 11, should provide such a measure. This is because $\Delta H°$(**2-X**) can be expected to depend in a similar way on the various factors discussed above for $\Delta H°$(**1-X**) except for the absence of aromaticity/antiaromaticity effects. In fact, not only do the $\Delta\Delta H°$ values show a remarkably good correlation with the ASE values (Figure 1), but also for the most part, the $\Delta\Delta H°$ and ASE values are numerically very similar to each other, with the exception of X = AlH; the unusually large $\Delta\Delta H°$ value for this system appears to be related to the anomalously high $\Delta H°$(**1-AlH**), which we have attributed to structural anomalies of **1H$^+$-AlH**.

$$\mathbf{1H^+\text{-}X} + \mathbf{2\text{-}X} \rightleftharpoons \mathbf{1\text{-}X} + \mathbf{2H^+\text{-}X} \qquad (11)$$

C. Barriers. The barriers, $\Delta H^{\ddagger}$, for reactions 5a and 5b are summarized in Table 6. In keeping with our previous studies we use the term barrier for the enthalpy difference between the transition state and the separated reactants rather than between the transition state and the ion-dipole complexes that precede the transition state in gas-phase ion−molecule reactions.[37] This is because those ion−dipole complexes have little relevance with respect to the questions addressed in this study.

Two sets of $\Delta H^{\ddagger}$ values are reported in Table 6; the first one is uncorrected ($\Delta H^{\ddagger}$), and the second is counterpoise-corrected ($\Delta H^{\ddagger}_{corr}$) for the BSSE.[32] We shall focus our discussion on $\Delta H^{\ddagger}_{corr}$. However, because these corrections are quite similar in all cases, none of the qualitative conclusions of this article would change if the uncorrected values were used.

The dependence of the barriers on X is even more complex than that of the proton affinities. This is because not only is

(37) (a) Farneth, W. E.; Brauman, J. I. *J. Am. Chem. Soc.* **1976**, *98*, 7891. (b) Moylan, C. R.; Brauman, J. I. *Amer. Rev. Phys. Chem.* **1983**, *34*, 187.

TABLE 8. Effect of Various Factors on $\Delta H^{\ddagger}$[a,b]

factor	progress at TS[b]	effect on $\Delta H^{\ddagger}$
aromaticity of **1-X**	develops ahead of PT	↓
antiaromaticity of **1-X**	lags behind PT	↓
resonance of **1H$^+$-X**	lost ahead of PT	↑
charge delocalization in **1-X**	lags behind PT	↑
electron-withdrawing effect of X in **1H$^+$-X**	lost ahead of PT	↓
electron-donating effect of X in **1H$^+$-X**	lost ahead of PT	↑
polarizability effect of X in **1H$^+$-X**	lost ahead of PT	↑

[a] Arrows pointing up (down) mean increase (decrease) in $\Delta H^{\ddagger}$. [b] PT = proton transfer.

$\Delta H^{\ddagger}$ affected by the same factors that influence $\Delta H°$ such as aromaticity/antiaromaticity, resonance, inductive and polarizability effects, etc., but the different degree of expression of those factors at the transition state ("imbalance") adds to the complexity. Table 8 lists the types of imbalances expected for the various operating factors and their effect on $\Delta H^{\ddagger}$. Note that since in identity reactions such as reactions 5a and 5b each species acts both as a reactant and a product, the effect of the transition state imbalances on $\Delta H^{\ddagger}$ is doubled. For example, the aromaticity of **1-X** lowers $\Delta H^{\ddagger}$ because as **1-X** becomes a product, its development is ahead of proton transfer. However, there is an equal additional decrease in $\Delta H^{\ddagger}$ because the loss of aromaticity from **1-X** being protonated in the reverse direction lags behind proton transfer.[5a] In a similar way, the early loss of the resonance stabilization of **1H$^+$-X** as the reaction proceeds in the forward direction and the late gain in resonance stabilization as **1H$^+$-X** is being formed in the reverse direction contribute equally to an increase in $\Delta H^{\ddagger}$. Note that for simplicity in Table 8 only the imbalances that occur in the forward direction are described.

The description of charge delocalization in the formation of **1-X** as lagging behind proton transfer (Table 8), which implies that charge delocalization in converting **1H$^+$-X** to the transition state is ahead of proton transfer, is supported by the calculated NPA charges reported in Chart 2 as discussed above. Regarding the inductive and polarizability effects exerted by X on **1H$^+$-X**, they are all described as being lost ahead of proton transfer. This is a consequence of the early loss of delocalization, which pulls the positive charge away from the CH-group that is adjacent to X as shown, in exaggerated form, in **7**. Evidence for this also comes from the NPA charges (Chart 2). They show that at the transition state the decrease in the charge on the CH group adjacent to X in **1H$^+$-X** has made more than 50% progress in all cases except for **1-AlH**. These percentages are 63.3 (**1-CH$^-$**), 55.3 (**1-NH**), 56.9 (**1-S**), 58.9 (**1-O**), 60.5 (**1-PH**), 53.9 (**1-PH**-(planar)), 62.1 (**1-CH$_2$**), 53.0 (**1-BH**) and 25.8 (**1-AlH**). The low percentage for **1-AlH** is another indication of the anomalous behavior of this system.

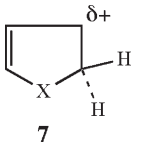

7

It should be clear from the above discussion that a quantitative or even semiquantitative evaluation of the contribution

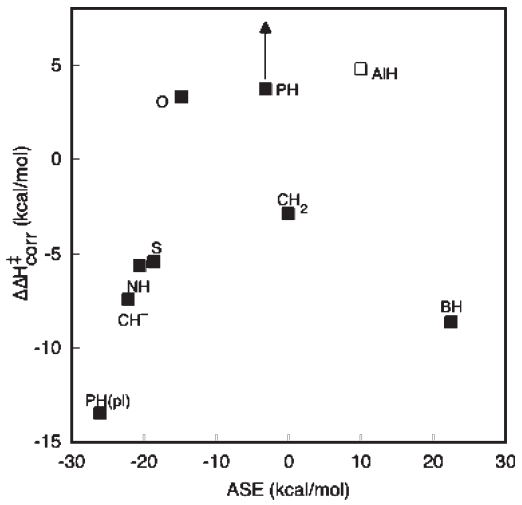

FIGURE 2. Plot of $\Delta\Delta H^{\ddagger}_{corr}$ versus ASE. The point for **1-AlH** (G) is anomalous (see text). The point for **1-PH** is probably lowered by an anomeric effect (see text).

of aromaticity/antiaromaticity to the $\Delta H^{\ddagger}_{corr}$ values would be very difficult and even more difficult than for the proton affinities as a result of the added complexity arising from the imbalanced nature of the transition state. Hence, a more promising approach, in analogy to the treatment of the proton affinities, is to focus directly on $\Delta\Delta H^{\ddagger}_{corr} = \Delta H^{\ddagger}_{corr}$(**1-X**) − $\Delta H^{\ddagger}_{corr}$(**2-X**), assuming that all factors except for aromaticity/antiaromaticity affect $\Delta H^{\ddagger}_{corr}$(**1-X**) and $\Delta H^{\ddagger}_{corr}$(**2-X**) in a similar way and hence essentially cancel out in $\Delta\Delta H^{\ddagger}_{corr}$. Figure 2 shows a plot of $\Delta\Delta H^{\ddagger}_{corr}$ versus ASE.

There are two legs on this plot, one for the aromatic systems with a positive slope and one for the antiaromatic systems with a negative slope. The general shape of the plot is what we would expect, i.e., both aromaticity and antiaromaticity lower the barrier (Table 8). The scatter in the plot on the aromatic side, which is worse than for the proton affinities (Figure 1), is probably due to a less than perfect cancelation of the various factors such as resonance, charge destabilization, inductive, and polarizability effects because the degree of the various imbalances could very well be different in the two reaction series. However, the point for **1-PH** may be too low because of a potential anomeric effect that lowers the barrier, as elaborated upon in the section on the NICS(1) values.

Conclusion

The results of the present study (reaction 5a) confirm earlier conclusions based on an examination of reactions 3a[17a] and 7[17b] as well as of some solution reactions,[13] i.e., in proton transfers that lead to an aromatic molecule or ion the development of aromaticity at the transition state runs ahead of the proton transfer. This early development of aromaticity leads to a lowering of the intrinsic barrier as required by the PNS for the early development of a product stabilizing factor,[4] and is in keeping with Nature's principle of always choosing the lowest energy path. As discussed in detail elsewhere,[4d,17a,38] the transition state aromaticity in our reactions should not be confused with the aromaticity of the transition state in pericyclic reactions such as [4 + 2] cycloadditions and others.[39] In these latter reactions aromaticity is mainly a characteristic of the transition state while the reactants and products are not aromatic or less so than the transition state and hence the low barrier is not a PNS effect.

Our results for the **1H$^+$-BH**/**1-BH** and **1H$^+$-AlH**/**1-AlH** systems also reenforce previous tentative conclusions that in proton transfers that lead to an antiaromatic product the development of antiaromaticity lags behind transfers.[17a,37] The result is again a lowering of the intrinsic barrier, as required by the PNS for the late development of a product *de*stabilizing factor and again consistent with the notion of choosing the lowest energy path. Note that this barrier-lowering effect is the opposite of the barrier enhancing effects in [2 + 2] cycloadditions and related reactions that have antiaromatic transition states[39] with barriers so high as to render the reactions to become "forbidden."

The way aromaticity and antiaromaticity affect intrinsic barriers is in marked contrast to the effects of resonance or charge delocalization, which lead to *increases* in intrinsic barriers because their development at the transition state invariably lags behind proton transfer.[4] The reason for this lag is that there are insurmountable constraints on how much charge delocalization is possible at the transition state, constraints that are related to the requirement of π-bond formation as the conduit for the charge delocalization.[4] Such constraints do not apply in the case of aromaticity; on the contrary, only relatively minor progress in the creation of the appropriate orbitals or their optimal alignment seems to be required for aromatic stabilization to become effective. For more elaborate discussions on this fundamental difference between how aromaticity and resonance/delocalization affect intrinsic barriers, refs 4d, 17a, and 39 should be consulted.

Calculations

Calculations were carried out using Gaussian 98[41] or Gaussian 03[42] on either a SUN X4200 2 x Opteron CPU, 8 GB RAM with 72 Gb disk space, or Sun Blade 1500 with SPARC process Solaris, 8 GB RAM with 490 Gb disk space.

Reactant and product neutrals and ions were drawn with ChemDraw and optimized first with MM2. Input for Gaussian 03 or Gaussian 98 were then prepared in Cartesian coordinates. Optimization was first done at the 3-21G* level and was followed by optimization at the MP2/6-311+G(d,p) level. Constraints for the planar phosphole and 1,3-butadiene-phosphine structures were introduced by the "add redundant" method (keyword addredun) for specifying fixed dihedral angles of 180.0° for the hydrogen atom(s) attached to the carbon chain or carbon ring.

Transition state structures required optimization via Z-matrix coordinates; Z-matrix construction exploited the proton as the center of symmetric inversion. Alternate Z-matrices were constructed to provide different starting points and to reveal

(38) Bernasconi, C. F.; Ruddat, V.; Wenzel, P. J.; Fisher, H. *J. Org. Chem.* **2004**, *69*, 5232.

(39) Bernasconi, C. F. *Pure Appl. Chem.* **2009**, *81*, 651.

(40) (a) Evans, M. G. *Trans. Faraday Soc.* **1939**, *35*, 651. (b) Dewar, M. J. S. *The Molecular Orbital Theory of Organic Reactions*; McGraw-Hill: New York, 1969; pp 316−339. (c) Zimmerman, H. *Acc. Chem. Res.* **1971**, *4*, 272.

(41) Frisch, M. J. et al. *Gaussian 98, Revision A.7*; Gaussian, Inc.: Pittsburgh, PA, 1998.

(42) Frisch, M. J. et al. *Gaussian 03, Revision D.01*; Gaussian, Inc.: Wallingford, CT, 2004.

unintended constraints. These alternate Z-matrices lead to identical energies and nearly identical geometric parameters. Optimization using Cartesian coordinates also demonstrated that the transition states presented are global minima. NICS(1) values for nonplanar structures required the determination of a minimum for the isotropic shift values above the structure with the appropriate sign change. For each such structure (all transition states, **1-PH**, **1H$^+$-BH**, **1H$^+$-AlH**, and the 1,3-butadiene-1,4-diylhydro system), three nonadjacent ring atoms were chosen, a set of ghost atoms arranged to span the structure 1 Å above the chosen plane. This process was repeated using different sets of nonadjacent atoms, three determinations made for each structure.

All MP2 calculations were carried out using the frozen core methods, the default for Gaussian 03. NICS(1) calculations are reported using the default, using the full correlation, and only the frozen core energies are reported. All vibrational modes were scaled[43] to obtain the zero-point energy and a thermal correction through the partition function of the vibrations. In all cases a basis set superposition error (BSSE) was calculated by the counterpoise method[33] and reported.

Acknowledgment. This research was supported by Grant CHE-0446622 from the National Science Foundation. We also thank Dr. Mark L. Ragains for some preliminary calculations and Stephen Hauskins for his administration of our computational platforms.

Supporting Information Available: Tables S1−S74 (detailed computational results), Table S75−S80 (geometries), Table S81 (energies), and Figures S1−S9 (geometric parameters). This material is available free of charge via the Internet at http://pubs.acs.org.

(43) Scott, A.; Radom, L. *J. Phys. Chem.* **1996**, *100*, 16502.